The influence of tow tackiness on tow pull-up during the manufacturing of a composite pressure vessel

Nedelcu, Alex; Florindo, André Mendes; Han, Sungi; Dekker, Jaap; Vlieger, Maarten de; Castro, Saullo G.P.; Peeters, Daniël

DOI
10.1016/j.mfglet.2024.03.011

Publication date
2024

Document Version
Final published version

Published in
Manufacturing Letters

Manufacturing Letters 40 (2024) 132–135

Contents lists available at ScienceDirect

Manufacturing Letters

journal homepage: www.elsevier.com/locate/mfglet

The influence of tow tackiness on tow pull-up during the manufacturing of a composite pressure vessel

Alex Nedelcu [a], Andre Florindo [b,*], Sungi H. Han [b], Jaap Dekker [c], Maarten de Vlieger [c], Saullo G.P. Castro [a], Daniël Peeters [a,b]

[a] *Faculty of Aerospace Engineering, Delft University of Technology, Kluyverweg 1, Delft, 2629 HS, The Netherlands*
[b] *SAM XL - Smart Advanced Manufacturing, Rotterdamseweg 382c, 2629 HG Delft, The Netherlands*
[c] *Airborne, Laan van Ypenburg 70, 2497 GB Den Haag, The Netherlands*

ARTICLE INFO

Article history:
Received 15 February 2024
Accepted 22 March 2024
Available online 2 April 2024

Keywords:
Automated fiber placement
Ritz method
Fiber steering
Tow pull up
Pressure vessels

ABSTRACT

Double-curved composite structures that are manufactured via automated fiber placement, such as pressure vessels, can take advantage of tow steering to reduce weight. This design freedom comes with the cost of adding internal normal stresses to the tow, possibly leading to wrinkles or pull up. The present work investigates tow pull up both experimentally and analytically and details a correlation between tow pull up and the minimum critical steering radius, where the material tackiness and the modelled plate's length are found to be the most influential parameters. The experimental determination of the material tackiness is the next step to improve the predictive capabilities of the proposed model.

1. Introduction

Lightweight composite pressure vessels have become a popular topic in recent years among aerospace companies while investigating ways to reduce emissions. One manufacturing approach involves Automated Fiber Placement (AFP) with tow steering.

In the frame of the ENVOL project [1], Airborne, in collaboration with SAM XL, produced a full-scale section of a pressure vessel, for an oxidizer tank of a small launcher, consisting of a cylinder-dome segment with tow steered layers, shown in Fig. 1a.

Before manufacturing this tank, initial trials were conducted to investigate the smallest steering radius that could be manufactured. These initial trials showed that tow pull-up was the predominant defect for low steering radii.

The physical phenomenon behind tow pull-up was presented in [2], however further research is needed to relate this phenomenon with process parameters and material characteristics. This work focuses on investigating the tow pull-up defect for two parameters: temperature and steering radius.

2. Material and methods

The experimental setup included an AFP head from ADDComposites AFP-XSGen2 attached to a KUKA KR210 manipulator, displayed in Fig. 1. The experiment consists of laying down quarter inch tows, with a constant steering radius on top of a flat substrate of a similar material to replicate the manufacturing conditions.

Two different materials are investigated, which due to confidentiality reasons will be referred to as Material 1 and Material 2. Both materials contain the same high tensile strength carbon fibers, but a slightly different thickness and thermoset resin: Material 2 has a resin content of 33 % and higher tackiness, thickness, and width compared to Material 1, which has a 35 % resin content. Both materials are based on TORAY TC700SC fibers and were outside their shelf life. Therefore, it is expected that both tows' tackiness are relatively decreased.

The experiments are divided into two steps. Initially, low heating is applied and the steering radius increased from 0.5 to 2 m in increments of 0.5 m. Later, a higher heat setting is used and steering radii are varied from 1 to 2 m with 0.2 m increments, keeping an arclength of 1 m. Layup speed and compaction forces are kept constant at 0.05 m/s and 375 N, respectively.

From the experiments, the resulting tow pull-up is visually characterized and divided into 4 categories, displayed in Fig. 1b-e:

- Perfect results: No visual pull-up, the tow is completely adhered to the substrate.
- Pull-up at start: the tow shows pull-up at the start, but further along is adhered perfectly.
- Sizeable pull-up: over a big part of the tow, it is being pulled up.

* Corresponding author.
E-mail address: a.m.mendesflorindo@tudelft.nl (A. Florindo).

https://doi.org/10.1016/j.mfglet.2024.03.011

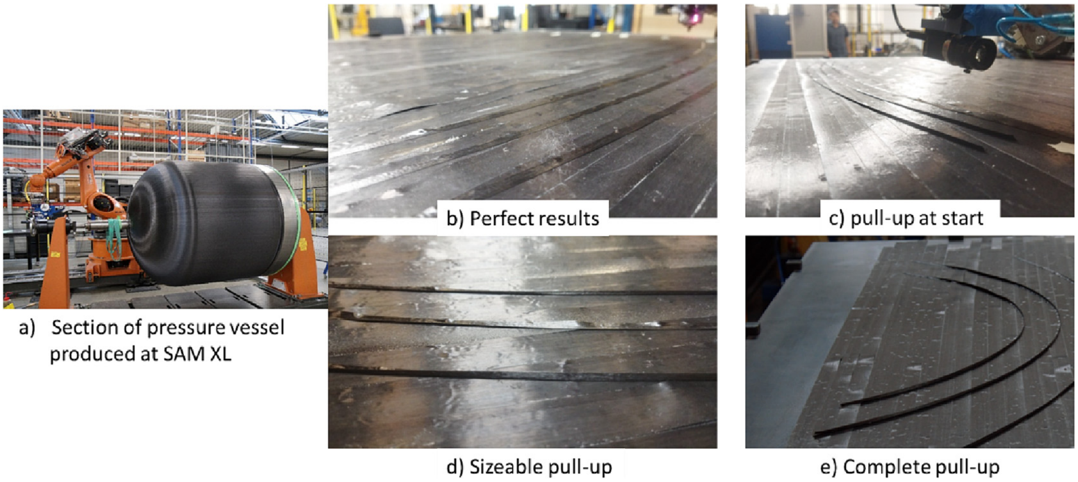

Fig. 1. AFP results: the overall pressure vessel and different tow pull-ups observed.

- Complete pull-up: all along the tow, the outer edge is lifted from the substrate.

Fig. 2 summarizes the observed pull-up for different steering radii and heating on both materials. In this figure, it is observed that the higher tackiness of Material 2 has a positive effect on the minimal achievable steering radius. Furthermore, the higher heating improves the achievable steering radius.

3. Calculation

The analytical model is built on the local approach used successfully in literature to model tow wrinkling [3–5], while studying the outer, rather than the inner, part of the tow. This approach models the defect as a rectangular orthotropic plate of length a, width b, and thickness h, on an elastic foundation with normal stiffness k.

Following literature, the Kirchhoff-Love hypothesis and the von Kármán approximation are used: normals to the mid-plane are assumed to remain normal, and in-plane effects are assumed to be negligible compared to the out-of-plane deflection w. The plate model and coordinate system is shown in Fig. 3b. This figure also shows the in-plane load P_y, which is caused by the curvature of the tow. While steering, there is a mismatch between the length of the outer side of the tow, where a maximum load P_0 occurs, and the length of the layup path (in the tow center), leading to a linearly varying load:

$$P(y) = P_0\left(1 - \frac{\alpha y}{b}\right) \tag{1}$$

which is controlled by a load parameter α. The value chosen for α is 2, meaning the load varies linearly from 0 to its maximum.

As observed in Fig. 3a, if the length at tow center is L_0, the radius of curvature is R and angle θ, the length on the outer side L is

$$L = \theta\left(R - \frac{b}{\alpha}\right) \tag{2}$$

Therefore, a strain exists in the outer part, which using Hooke's law, assuming an elastic modulus E_1, can be converted to a stress. By multiplying with the thickness h, the maximum value of the distributed load is found to be

$$P_0 = \frac{E_1\, h\, b}{\alpha R} \tag{3}$$

Next, the Rayleigh-Ritz energy method is applied to this orthotropic plate. The functional Π is composed of the elastic strain energy U, the potential (elastic) energy of the foundation K, and the work done by the in-plane loading Q:

$$\Pi(w) = U(w) + K(w) - Q(w) \tag{4}$$

The strain bending energy U is defined as

$$U(w) = \frac{1}{2}\int_0^a \int_0^b D_{11}\left(\frac{\partial^2 w}{\partial x^2}\right)^2 + D_{22}\left(\frac{\partial^2 w}{\partial y^2}\right)^2 + 2D_{12}\frac{\partial^2 w}{\partial x^2}\frac{\partial^2 w}{\partial y^2} + 4D_{66}\left(\frac{\partial^2 w}{\partial x \partial y}\right)^2 dydx \tag{5}$$

where D_{ij} are the out-of-plane stiffness terms obtained from classical laminate theory.

The elastic potential energy K is given by

$$K(w) = \frac{1}{2}\int_0^a \int_0^b k w^2\, dy\, dx \tag{6}$$

where k is the normal stiffness of the elastic surface.

The work Q is defined by

$$Q(w) = \frac{1}{2}\int_0^a \int_0^b P\left(\frac{\partial w}{\partial x}\right)^2 dydx \tag{7}$$

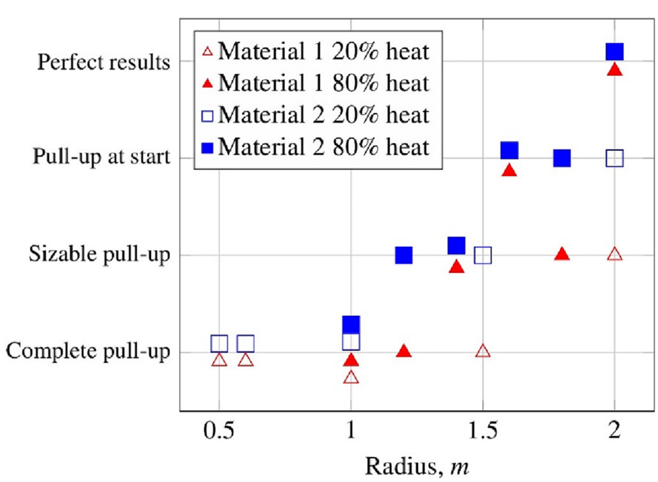

Fig. 2. Pull-up results observed during experiments for different materials, steering radii and heating.

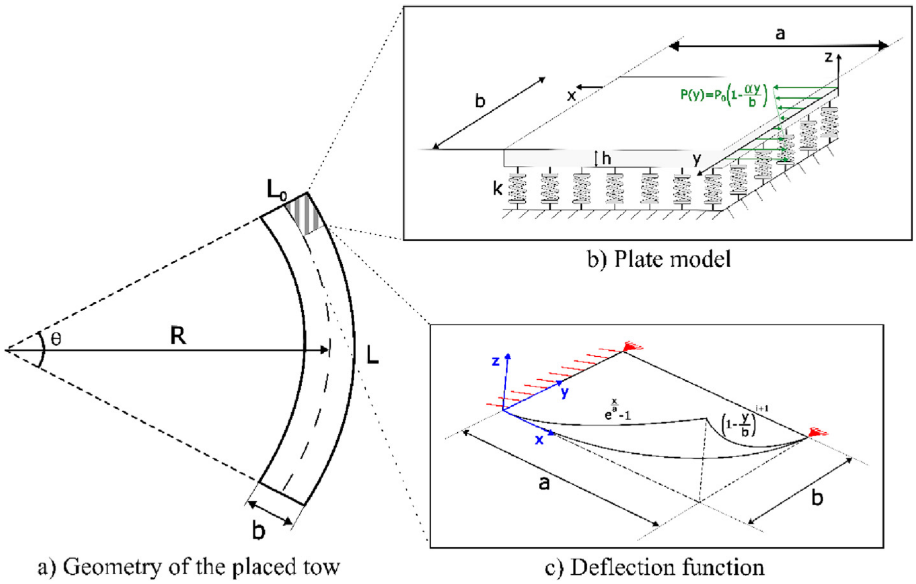

Fig. 3. Description of the tow geometry and representation of the plate model and deflection function.

The pull-up phenomenon is treated as a tensile buckling scenario, which occurs when the functional Π is minimized, mathematically when

$$\frac{\partial \Pi}{\partial a_i} = 0 \tag{8}$$

As deflection function w, we found that a function comparable to the observed defect shape at the start, shown in Fig. 3c is

$$w(x,y) = \sum_{i=1}^{n} a_i \left(1 - \frac{y}{b}\right)^{i+1} \left(e^{\frac{x}{a}} - 1\right) \tag{9}$$

This function can be substituted into the previous equations, and using n = 1, the critical maximum load is found to be

$$P_{0_{cr}} = \frac{2}{6-\alpha}\left(\frac{3D_{11}}{a^2} + \frac{14.236D_{22}a^2}{b^4} + \frac{59.05D_{12}}{b^2} + \frac{80D_{66}}{b^2} + 0.712ka^2\right) \tag{10}$$

The critical radius related to this load is found to be

$$R_{cr} = \frac{E_1 hb(6-\alpha)}{2\alpha} \times \frac{1}{\frac{3D_{11}}{a^2} + \frac{14.236D_{22}a^2}{b^4} + \frac{59.05D_{12}}{b^2} + \frac{80D_{66}}{b^2} + 0.712ka^2} \tag{11}$$

4. Results

As an initial sensitivity analysis of the model to its input, we used a baseline, and varied the different parameters from this baseline, one at a time. The values used are based on literature and the modulus of the fibers, the resin properties have not been taken int account. The following data have been used:

- a: 13 mm (varied from 5.6 to 20 mm)
- k: 109 N/m3 (varied from 2.5*108 to 1.8*109 N/m3)
- E_1: 152.5 GPa (varied from 145 to 160 GPa)
- E_2: 1.2 GPa (varied from 0.046 MPa to 2.4 GPa)
- G_{12}: 1.552 GPa (varied from 0.079 MPa to 3.825 GPa)
- ν_{12}: 0.3 (varied from 0.2 to 0.42)
- ν_{21}: 0.02 (varied from 0 to 0.05)

The results can be seen in Fig. 4. Clearly, the length and foundational stiffness have the largest influence on the critical radius. To determine the length a, we re-investigated the tests and noticed that after about 10 mm the tape started to peel off, so this length is chosen. The elastic stiffness is still under investigation, but as both materials were out of shelf life, it is expected to be on the lower side of the checked range, leading to a larger critical radius.

5. Discussion

When comparing the baseline value of the model to the observed test results, it can be observed that the order of magnitude matches with the observed pull-up. Indeed, the material with lower tackiness (elastic stiffness foundation) had a critical radius of 2 m with high heating. For the high tackiness material, a slightly better behavior is observed in general, where a critical radius of about 1.8 m is found.

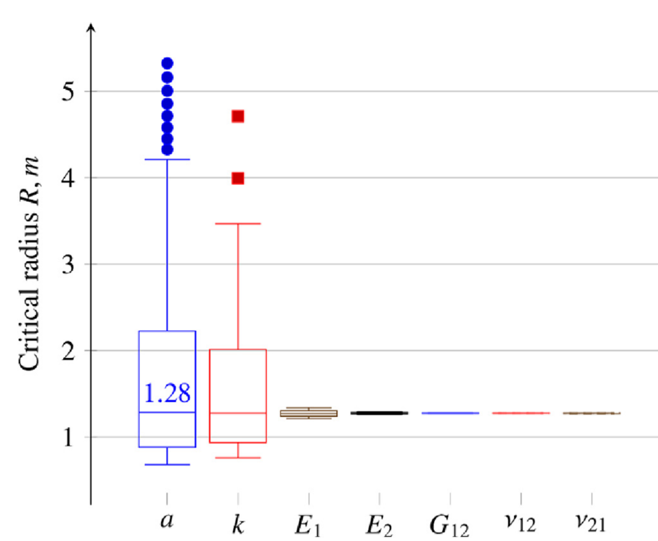

Fig. 4. Sensitivity study on the different model parameters for Material 1.

6. Conclusion

This work presented an analytical method to predict the critical radius for tow pull-up. The model gave results in the correct order of magnitude for the critical radius, but unfortunately the material tackiness could not be measured accurately yet. However, the sensitivity analysis clearly shows that the material tackiness and plate length are the most important model parameters. Future experimental efforts in determining the material tackiness should enable the model herein proposed to predict the critical radius for tow pull-up in fiber steered composites.

CRediT authorship contribution statement

Alex Nedelcu: Methodology, Validation, Investigation, Visualization, Writing – original draft. **Andre Florindo:** Writing – review & editing. **Sungi H. Han:**Software, Investigation, Writing – review. **Jaap Dekker:** Writing - review. **Maarten de Vlieger:** Resources, Writing – review. **Saullo G.P. Castro:** Supervision, Writing – review. **Daniël Peeters:** Conceptualization, Supervision, Writing – review & editing.

References

[1] https://envol-h2020.eu/.
[2] Bakhshi N, Hojjati M. An experimental and simulative study on the defects appeared during tow steering in automated fiber placement. Compos A Appl Sci Manuf 2018;113:122–31.
[3] Beakou A, Cano M, Cam J-B-L, Verney V. Modelling slit tape buckling during automated prepreg manufacturing: a local approach. Compos Struct 2011;93:2628–35.
[4] M.Y. Matveev, P.J. Schubel, A.C. Long, and I.A. Jones, ''Understanding the buckling behaviour of steered tows in automated dry fibre placement (adfp),'' Composites Part A: Applied Science and Manufacturing, vol. 90, pp. 451–456, 11 2016.
[5] M. Belhaj and M. Hojjati, ''Wrinkle formation during steering in automated fiber placement: Modeling and experimental verification,'' Journal of Reinforced Plastics and Composites, vol. 37, pp. 396–409, 3 2018.